Radiation Damage Analysis for the ESS Target

February 9, 2016

Reference:	ESS-0037287
Date:	February 9, 2016
Revision:	1.0

Authors	Review	Aproved
F. Sordo (ESSB) A. Ghiglino (ESSB) L. Mena (ESSB) A. Aguilar (ESSB) T. Mora (ESSB) I. Herraz (ESSB) R. Vivanco (ESSB) M. Magan (ESSB) M. Mancisidor (ESSB) J. de Vicente (ESSB) F.J. Bermejo (CESIC) J.L. Martinez (ESSB)	F. Sordo (ESSB)	J. L. Martinez (ESSB)

Contents

1 Introduction

Spallation sources are devices designed to produce neutrons from nuclear reactions. In order to produce this kind of reactions it is necessary to accelerate a proton using electromagnetic fields up to a huge amount of kinetic energy. At that moment, protons are led to impact on a nucleus of a heavy atom (generally mercury, lead or tungsten) producing what it is known as a spallation reaction.

The place where the reaction is produced is known as Spallation Target and it is considered the neutron source. These Targets are complex devices from an engineering point of view, where a huge amount of heat is deposited in the spallation material. It is worth noting than in some cases, the heat density can be higher than fuel bars in a nuclear power reactor, making an equivalent engineering challenge. ESS target is one of these cases.

The European Spallation Source is an ambitious European project with a budget over 1800 M€. The aim is to build the most important and the greatest spallation source in the world. It will use a proton beam with 5 MW final power (five times higher than SNS and JPARC) which will impact on a tungsten Target cooled by helium gas.

The Target will be designed with a set of tungsten blocks placed inside of a wheel of 2.5 meter of diameter. Protons imping on the wheel from a radial direction. Inside the wheel, helium flows at high velocity, cooling the tungsten blocks and dissipating the heat produced by the nuclear reactions. The wheel rotates at a speed of 0.2-0.5 Hz, so the proton beam impacts on a different region of the wheel, distributing the heat over the whole perimeter and volume.

Protons and neutrons generated by spallation reactions will produce a high radiation environment on the Target wheel. This environment leads to changes in material properties that could lead to the mechanical failure of the component, hence why this evaluation of radiation damage is one of the critical steps in the design process of such devices. The aim of this report is to evaluate the radiation damage produced in the ESS Rotating Target.

2 Irradiation damage: Basic issues

Spallation targets operate in very high radiation environment arising from both the constant bombardment of the proton beam and the neutrons and other particles and nuclear fragments generated by the spallation reactions. There are four different issues to be considered as sources of radiation-induced damage such as:

- Electronic excitations: When an ion transfers its energy to material electrons an ionization process takes place. In the case of metals, the energy given to the electrons is distributed between all the system as heat without leading to significant damage. In contrast, ionization within isolators like ceramics or polymers may easily severe chemical bonds thus producing a fast degradation of the material.
- Collisions: when an energetic particle collides with nuclei transmits part of its incoming energy. If the energy transmitted is higher than the threshold energy of the crystalline net the atom moves from its position, generating a Primary Knockdown Atom (PKA). This PKA can produce additional collisions with other atoms and move them from their positions. This effect is known as displacement cascade.
- Nuclear reactions: if the incident particle has enough energy, nuclear reactions can take place. In such nuclear interactions a large amount of energy is transmitted to the reaction products, generating high energy recoil nuclei. As in the previous cases this recoiling particles can produce a displacement cascade.
- Gas production: An special case of nuclear reaction is the production of light gas isotopes (H_2 or He). These gases are produced in large quantities on materials under high energy particles irradiation and typically accumulates inside the material. If the gas accumulation is high enough it leads to swelling.

Steel and Tungsten are metallic materials so the ionization effect can be ignored. Nevertheless, the other components of the damage could have an important effect in the mechanical properties. In the following sections a review of the damage analysis methodology is given. After than, the described methodology will be applied to the ESS target damage analysis.

3 Methodology

3.1 Displacement cascades

When an atom receives an amount of energy larger than the displacement threshold energy of its lattice, the atom moves from its equilibrium position to an interstitial thus leaving a vacant site. This combination of an atom in an interstitial position, called Self-interstitial-atom, (SIA) and a vacant is known as *Frenkel Pairs*. The kinematics of the displacement cascade is described below, ignoring relativistic effects. In an elastic collision, the maximum energy transfer from an incident particle (1) to a static particle (2) is:

$$E_m = \frac{4E_0 A_1 A_2}{(A_1 + A_2)^2} \tag{1}$$

Where A_1 and A_2 are the atomic masses of the particles. In the case of a neutron or proton hitting a heavy material such as Iron, $E_m \sim 4E_0 A^{-1}$. Alternatively, if $A_1 = A_2$, any energy up the full energy of the incident particle may be transfered. This is the case when a PKA hits another atom of the lattice.

When the average energy transmited by neutrons the media atoms is relative high, the PKA atom lose its electrons and performs as an ion. Its capacity to produce additional displacements in the atoms of the metallic mesh is limited by its interaction with the electrons of the media. There are two important thresholds to highlight: the threshold to remove an electron of the media and threshold to move an atom to its position in the net.

The first limit is the energy needed to remove an electron from the media (energy cut-off). This energy is proportional to the atomic number of the element (2). Above this energy, most of the energy transmitted to the PKA is lost by interactions with the electrons of the media so, for metallic materials as iron, this fraction of the energy not produce damage additional displacements.

$$E_c \sim 10^3 A(eV) \tag{2}$$

The second important threshold is the energy needed to move and atom to and interstitial position in the net. Typically this energies are between 40 to 90 eV per displacement. Below this limit, the PKA can not displace additional atoms of the net. The Table 1 shows the standard displacement energies proposed by ASTM/E for most common elements [3].

Element	Be,C	Al	Fe,Co,Ni	W, Ta
T_{th} (eV)	31	25	40	90

Table 1: Threshold energies for common elements

Based on this two critical energies, several models have been proposed to calculate the total number of atoms displaced by a given PKA based on its energy. Early on, the Kinchin and Pease model is used[2]. This model is based on the hypothesis that between a threshold energy and an upper energy cut-off, the number of Frenkel pairs generated follows a linear relationship with the energy of the incident particle. Below the threshold, no displacement is produced (though neutrons can still cause damage by other mechanisms), and above the upper cut-off, the additional energy is assumed to be dissipated by electronic excitation.

Back in the sixties, Linhard developed a more detailed theory calculating the fraction of the PKA energy that was dissipated in electronic excitations [?]. Norgett, Robinson and Torrens (NRT) developed, using this theory, the NRT model. This model gives the total number of displaced atoms produced by an PKA as:

$$\nu_{NRT}(T_i) = 0.8 \cdot \frac{T_i \cdot L(T_i)}{2 \cdot T_{th}} \tag{3}$$

$$L(T_i) = \frac{1}{1 + k \cdot g(\epsilon)} \tag{4}$$

where T_i is the energy of the PKA, T_{th} is the displacement threshold energy and k and $g(\epsilon)$ are efficiency factors as a function of the PKA energy. The 0.8 factor in the equation accounts for the fact that atoms are not actually hard spheres. We have to remark that ν_{NRT} is the "useful energy" to produced displacements in the net but, a fractions of this displacements will recombine after the damage so, this value is useful for damage comparisons but it is not an observable magnitude.

The parameters k and $g(\epsilon)$ can be obtained by the following equations:

$$k = \frac{0.0793 \cdot Z_i^{2/3} \cdot \overline{Z}_{target}^{1/2} \cdot (A_i + \bar{(}A)_{target})^{3/2}}{(Z_i^{2/2} + \overline{Z}_{target}^{2/4} \cdot A_i^{3/2} \cdot \overline{A}_{target}^{1/2})} \tag{5}$$

$$g(\epsilon) = \epsilon + 0.40244 \cdot \epsilon^{3/4} + 3.4008 \cdot \epsilon^{1/6} \tag{6}$$

$$\epsilon = \alpha \cdot T_i \cdot 10^6 \tag{7}$$

$$\alpha = \frac{0.8853 \cdot \overline{A}_{target}}{27.2 \cdot Z_i \cdot \overline{Z}_{target} \cdot (Z_i^{2/3} + \overline{Z}_{target}^{2/3})^{1/2} \cdot (A_i + \overline{A}_{target})} \tag{8}$$

The NRT model is widely used for the evaluation of radiation damage and we will adhere to it. Nevertheless, this model does not consider the recombination of the Frenkel pairs produced so, despite of the fact that the numbers obtained are comparable with the bibliography, they can not be directly correlated with the experimental observations.

3.2 Displacement Cross-section

The methodology described in the previous section shows the process to evaluate the number of displacements starting from the PKA energy. The energy transmited by a neutron to the PKA can be evaluated directly from the cross section:

$$T_i(E,\mu) = \frac{A \cdot E}{(A+1)^2} \cdot (1 - 2 \cdot R \cdot \mu + R^2) \tag{9}$$

where μ is the scattering cosine and the R is given by:

$$R = \sqrt{1} - \frac{(A+1) \cdot (-Q)}{A \cdot E} \tag{10}$$

The Damage production cross section is then obtained from:

$$D(E) = \sigma(E) \int_{-1}^{1} f(E,\mu) T_i(E) \cdot \nu_{NRT}(T_i) d\mu \tag{11}$$

where f is the angular distribution from the ENDF/B [4]cross section.

The described methodology has been applied by KIT team[1] for the production of damage cross section for neutrons and protons. Based on the following procedure the DPA ratios has been evaluated for neutrons and protons:

$$DPA_{NRT} = \int_{0}^{2GeV} \Phi_n(E) \sigma_{DPA}(E) dE \tag{12}$$

The Figure 1 shows the damage cross sections for Iron up to 2 GeV energy. We can remark that low energy protons do not produce a significant amount of damage compared with hight energy ones so, the simulations can be cut at 10^{-4} MeV in order to save computing time.

The coincidence in the damage cross section at hight energy level for both particles means that (model description shown on section3.1) that the PKA spectra produced is similar and so damage produced is comparable.

3.3 Gas production cross-section

The second parameter that leads the radiation damage conditions is the gas production. Most of the materials under high energy neturons irradiation generate significant amounts of hydrogen and helium. These light species can migrate in the metallic network to interstitial positions or boundaries between grain boundaries producing gas bubbles

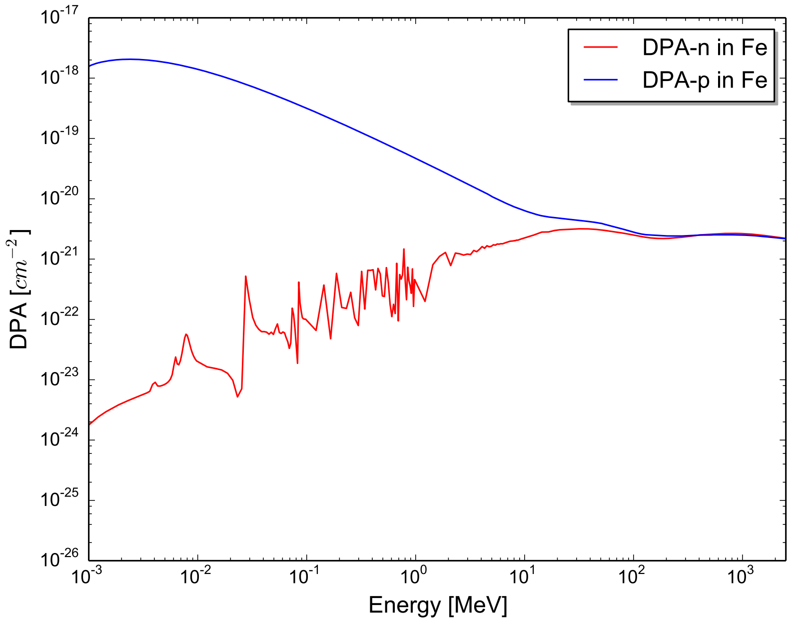

Figure 1: Damage cross section for neutrons and protons on iron

inside the material. These bubbles can increase the macroscopic dimensions of the material in a phenomena known as shelling. The Figures 2 and 3 shows the gas production cross section.

In most of the metallic elements hydrogen is light enough to migrate up to surface of the material and the shelling effect is lead by the helium accumulation. As shown on Figure 3, the helium production cross section for protons above 10 MeV is very similar to the cross section for neutrons so both particles will produce the same helium distribution inside the material.

3.4 Considerations for neutron damage on RCC-MRx design code

The standard design codes for pressurized equipment on nuclear environment (ASME or RCC-MRx) establish criteria for the utilization of materials under radiation environment. Typically these criteria give a relation between the irradiation damage and the acceptable stress level in order to limit the solicitations for the materials.

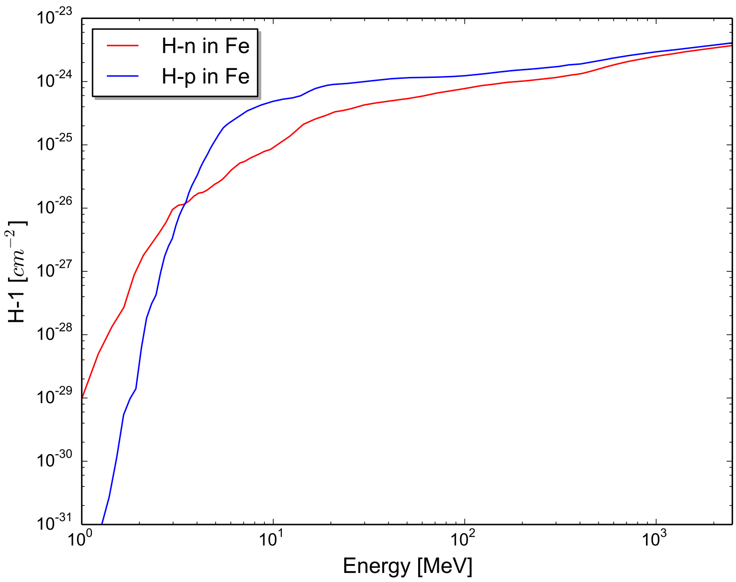

Figure 2: Hydrogen production cross section for neutrons and protons on iron

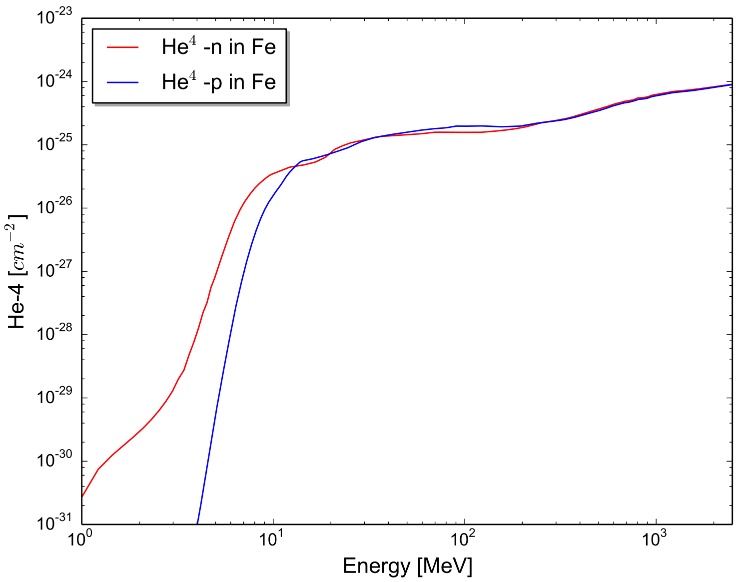

Figure 3: Helium production cross section for neutrons and protons on iron

The the reference code for ESS (RCC-MRx[8]) has been developed for neutron radiation damage on fusion and fission applications. This means that the materials have been tested for neutrons up to 14 MeV. In the case of ESS Target, the maximum neutron energy rises up to 2000 MeV hence, it is not obvious that the damage produced by spallation neutrons can be covered by the code.

If we considered an elastic collision between a neutron and an static atom, the average energy transmitted to the PKA is given by the following expression[7]:

$$< E_{PKA} >= E_{neutron} \cdot \frac{(1-\alpha)}{2} \tag{13}$$

$$\alpha = (\frac{A-1}{A+1})^2 \tag{14}$$

where A is the mass number of the PKA. Considering an iron atom, the average energy of the PKA is $\sim$ 3.5 % of the neutron incoming energy.

In order to compare the damage produced by 2-14 MeV neutrons (covered by the code) and 200-2000 MeV spallation neutrons we have to consider that the average energy of the PKA produced by these neutrons are respectively 70-490 keV and 7-70 MeV. Figure 6 shows the damage displace efficiency as a function of the PKA energy based on the Linard-Robinson model described on previous sections. This function represents the fraction of energy of the PKA which it is not dissipated by electron interactions and can produce displacement.

The Table 2 shows the energy values for the average collision for neutrons at 2,14,30, 200 and 2000 MeV. Neutrons at 30 MeV produce damage cascades with only a 20% more energy than 14 MeV, hence, the density and shape of the damage cascade (Figure 3 on [5]) have to be similar. Figures 4 and 5 shows two cascades in copper produced by 200 and 1000 keV[]. The cascade produced by 1000 keV is similar to 5 cascades of 200 keV communicated by areas with low displacement densities (the path of the primary recoil) so the damage effect can be considered as linear. It should be remarked that more than 95 % of the neutron displacement damage in the target is produced by neutrons with energies below 30 MeV (see Section 5.2).

To conclude this analysis, note that the final energy available to produce displacement for the high energy spallation neutrons is only a factor of 2 higher that the 14 MeV, hence not enough to change dramatically the structure of the damage cascades.

Taking into account this similarities in the available damage energy between fussion neutrons and “spallation neutrons”, we can conclude than the evaluation process proposed

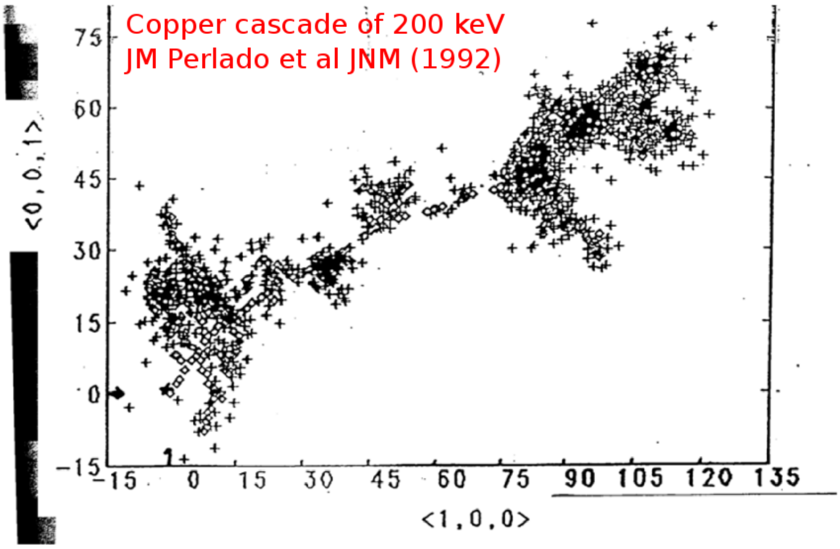

Figure 4: Displacement cascade produced by 200 keV copper on copper[6]

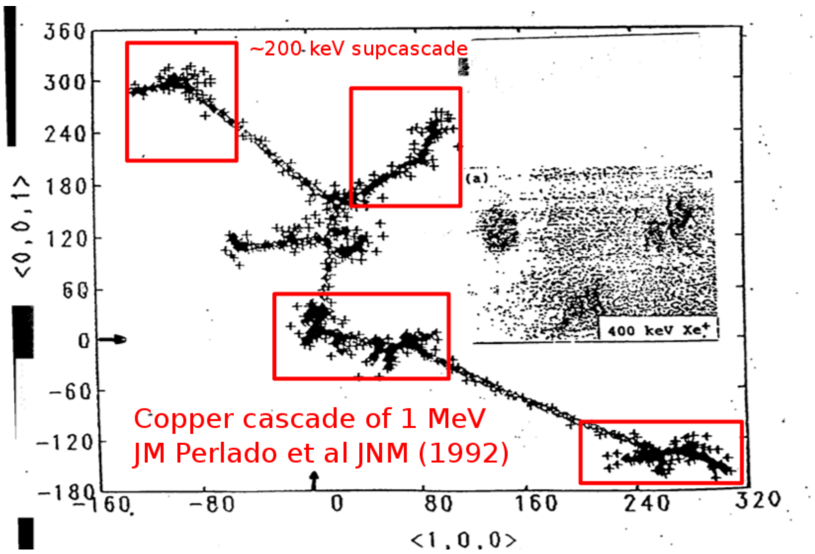

Figure 5: Displacement cascade produced by 1 MeV copper on copper[6]

by RCC-MRx developed to fussion-fission neutrons is acceptable to evaluate the material performance for spallation neutrons.

As summary of the previous discussion, we can conclude that the DPA pro-

Neutron Energy (MeV)	Averaged PKA (MeV)	Damage displace efficiency $L(T_i)$	Displacement Energy (keV)
2	0.070	0.52	36.5
14	0.490	0.25	124.0
30	1.050	0.16	164.7
200	7	0.033	230.9
2000	70	0.0037	258.3

Table 2: Threshold energies for common elements

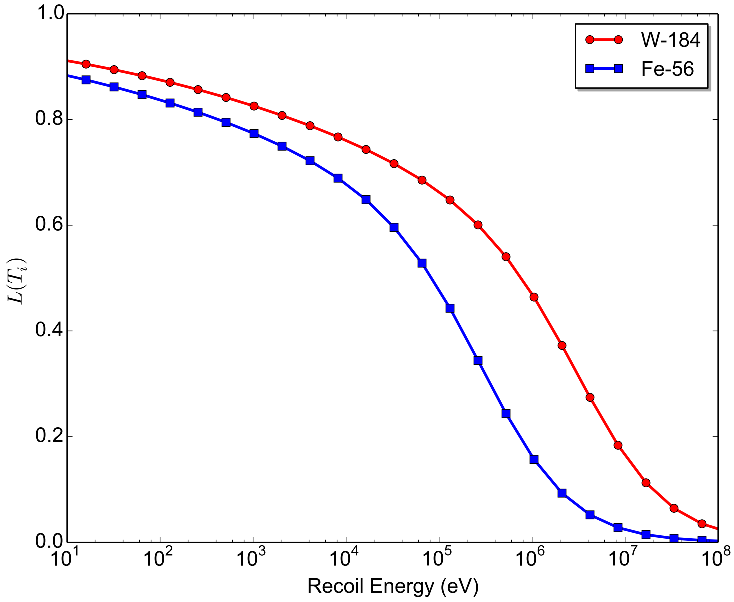

Figure 6: Damage displace efficiency as a function of the PKA energy

duced by "spallation neutron" is comparable with fussion DPA and based on that no additional safety factor is needed for RCC-MRx material limits.

We have to remark that the previous discussion had not taken into account the gas accumulation which also plays a role in the material performance under radiation. Hence, the ratio between He and DPA also have to be evaluated on each particular case to be under safe conditions.

3.5 Considerations for proton damage on RCC-MRx design code

Proton damage is not cover by RCC-MRx code. However, it the case of high energy protons damage there similarities with high energy neutrons that should be remarked.

The main diference between damage cascades produced by ions and neutrons is that ions has a very hith interaction cross section. This means that they can produce several PKA atoms close in the space and so there are interaction effects between two diffrente PKA cascades. However, in the case of neutrons the mean free path of the particle between collisions is in the range of $\sim cm$ whereas the size of the cascade is in the sub μm range, hence, there is no interaction between cascades.

The protons crossing the beam entrance window has an energy of 2000 MeV. We should take into account that for proton energies above 100 Mev, the coulom barrier effects are negligible, hence the mean free path of the particle in between collisions is also in the $\sim$ cm range. Due to this, for these high energy protons there is no interaction effect in between cascades.

Based on this effect, the proton performs in a very similar way to a high energy neutrons. Of course, the proton loses a significant amount of its energy due to electronic interactions. However, this energy will not produced damage in metals, so if a direct collision is produced, the elastic scattering analysis proposed in the previous section is a good approximation to estimate the energy of the PKA produced. Therefore the values shown on Table **??** for 2000 MeV neutrons can be applied to 2000 MeV protons.

Therefore the structure of the displacement cascades produced by protons in the beam entrance window will have double the size of the fusion damage cascades. The simulation analysis shows that there are even larger differences in the damage available energy can be found comparing fussion and fision recoils [5] and both of then are included in the RCC-MRx rules as the same type of "dpa". Hence there is no reason to consider that the high energy protons cascades needs any additional safety factor.

Once again, we have to remark that the previous discussion had not taken into account the gas accumulation which also plays a role in the material performance under radiation. Hence, the ratio between He and DPA also have to be evaluated on each particular case to be under safe conditions.

3.6 Considerations about life time of the target

The previous analysis was focused on the damage analysis to compared with the mechanical design rules for equipment under pressure but the life time of the target is not under the scope of previous analysis. Additional information can be found on ESS Material Handbook [14].

4 Particle transport model

In order to evaluate the particle distribution wheel needed to solve Damage formulation (15) MCNP6[9] code is used. This code is the latest version of MCNP family codes for montecarlo particle transport developed by Los Alamos National Laboratory in USA.

The MCNP model for the target wheel has been generated from the CATIA 3D model [10] by means of CADtoMCNP tools [11] and [12]. This means that the model reproduces with high accuracy the geometry of the target components. However, the model is much more detailed than usually needed for neutronic analysis so it is only recommended for target wheel analysis.

Figures 7 and 8 show the MCNPX model for the target. A detailed geometry of 4 sectors has been included in order to produce high accuracy results for heat load, irradiation damage and streaming proton paths along the wheel. The remaining 32 sectors has been simplify as an homogeneous mixture of helium and tungsten keeping the average density.

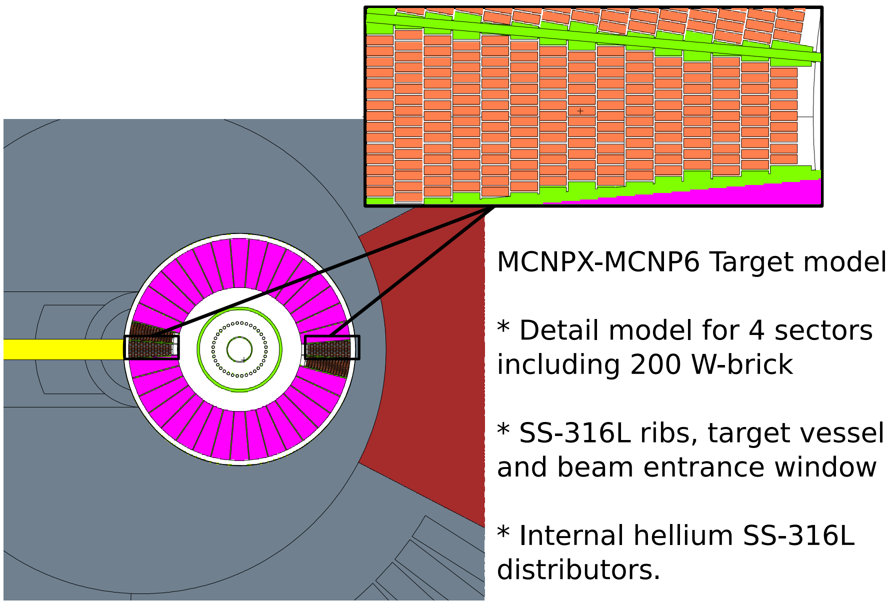

Figure 7: MCNP6 geometrical model for ESS Target.

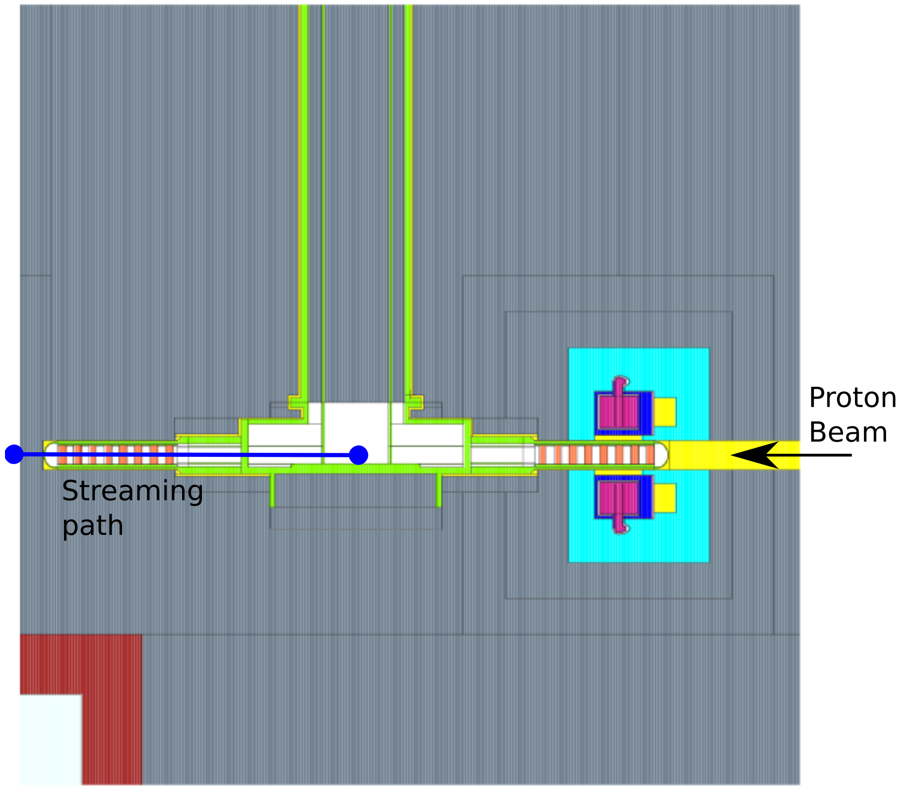

Figure 8: MCNP6 geometrical model for ESS Target.

5 Results

5.1 Damage on Spallation material

As it was mentioned in the introduction, the ESS Target will use tungsten as spallation material. This element is well known to became brittle with very small values of irradiation damage[13] so the evaluation of the irradiation conditions during operation is essential for the target design. However, tungsten is not an structural material in the wheel, hence, its failure is not associated with a loss in the pressure confinement barriers of the system.

The damage in the tungsten has two clear components: in one hand we have protons of the beam which produced the spallation reactions. The proton beam will hit each sector every 36 pulses, so the total damage is distributed in all the elements of the wheel. In order to evaluate the worst conditions from the irradiation point of view, we have assumed a perfect synchronization between the beam and the rotation of the wheel, so, the maximum proton beam current is always in the same position.

Figures 12, 13 and 14 shows the dpa, hydrogen and helium generation by proton flux.

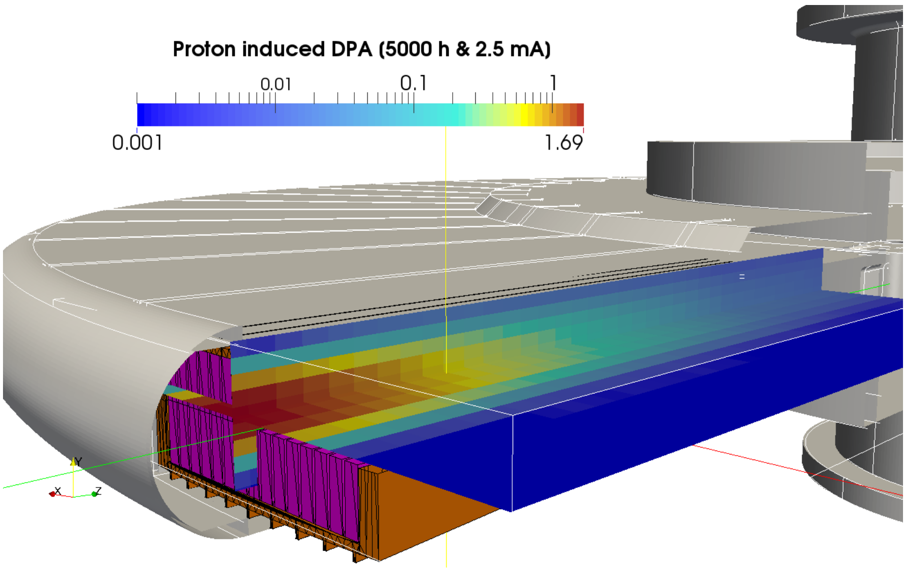

Figure 9: Proton induced damage (DPA) in the spallation material for 5000 h full power operation

The proton irradiation is produced only if the cassette is in front of the beam. Opposite to that, the neutron irradiation is produced also when the cassette is not in from of the beam due to the neutrons reflected by the moderator,reflector and shielding. To capture this effect in the analysis the neutron flux has been evaluated all along the angular movement in order to consider in the analysis all the contributions:

$$\overline{\Phi(E,r,z)} = \int_0^{2\pi} \Phi_n(E,r,\Psi,z)d\Psi \tag{15}$$

Figures 12, 13 and 14 show the damage produced by neutrons. It can be remarked that proton damage is a much higher than neutron damage, but neutron effect is not negligible. Notice also than neutron average energy is much lower than protons one so, despite neutron dpa is around 30% of protons one, in the case of gas production there is a factor of more than 10 between both.

In order to summarize both sources of damage, the Figures 15 and 16 includes the total values for damage and the ratio Helium/dpa. Along 5 years of full power operation, the

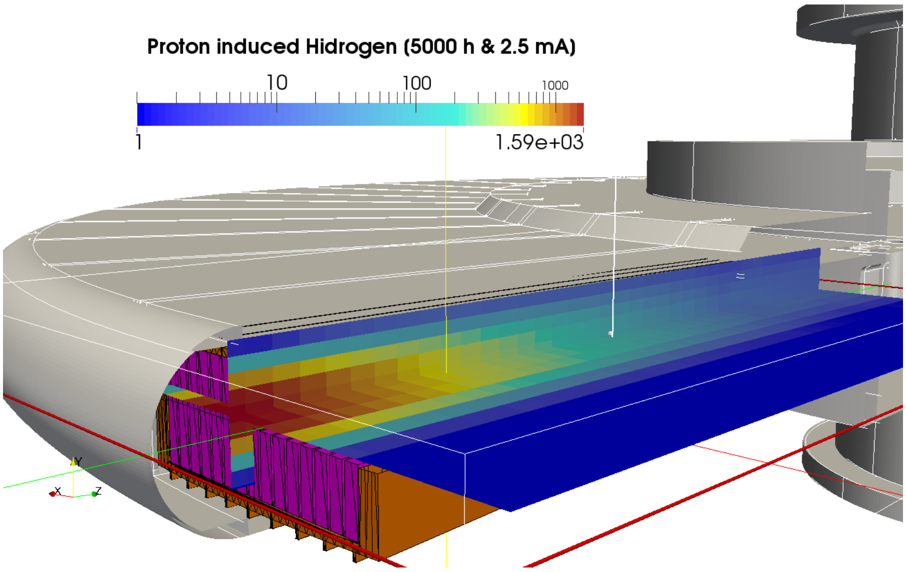

Figure 10: Hydrogen production by protons in the spallation material for 5000 h full power operation

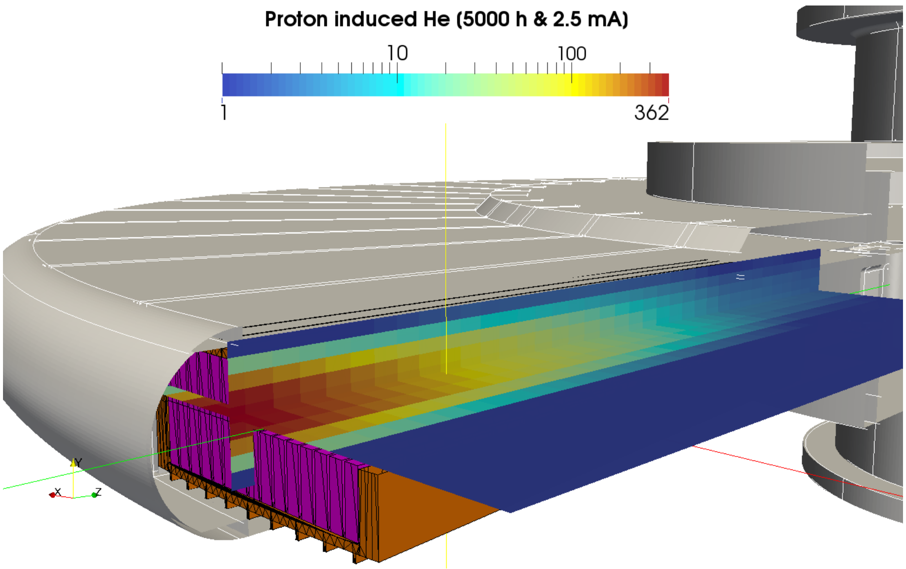

Figure 11: Helium production by protons in the spallation material for 5000 h full power operation

spallation material will accumulate 10 dpa and 2000 appm of helium. Based on the ESS

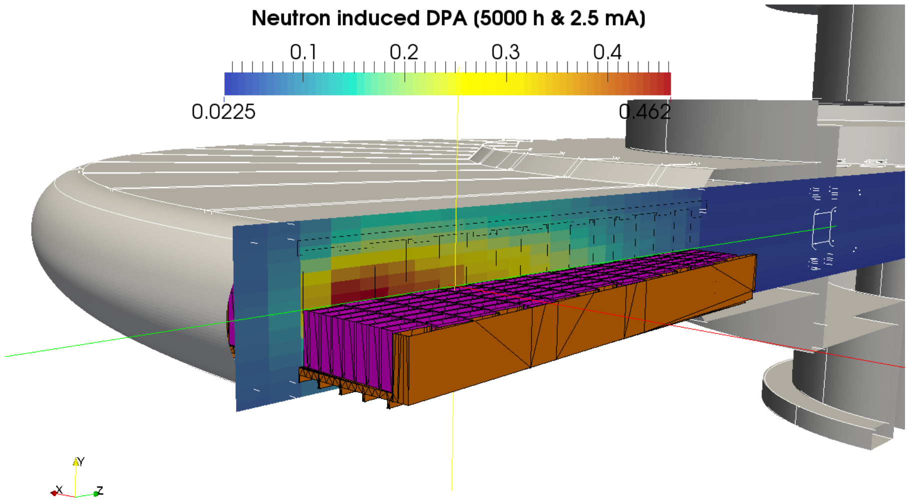

Figure 12: Neutron induced damage (DPA) in the spallation material for 5000 h full power operation

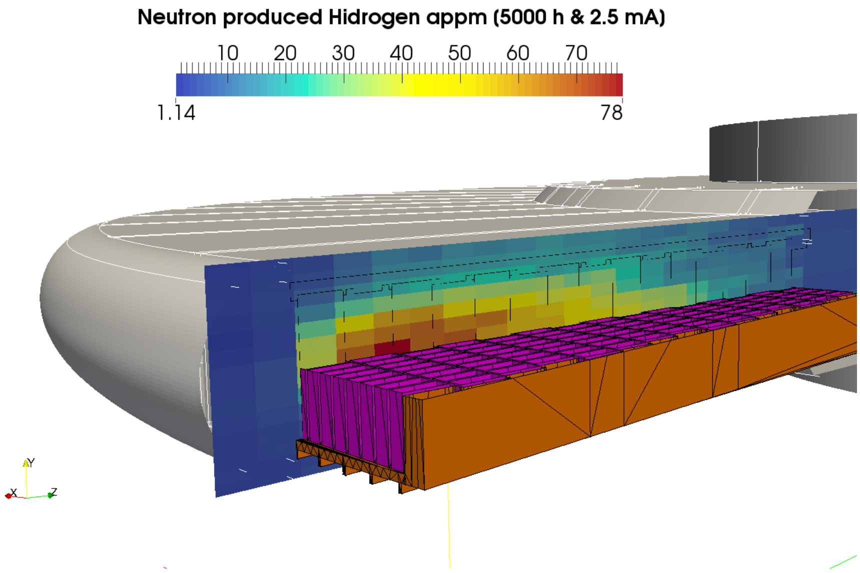

Figure 13: Hydrogen production by neutrons in the spallation material for 5000 h full power operation

Material Handbook [14] we should expect a 0.22% increase of volume due to swelling

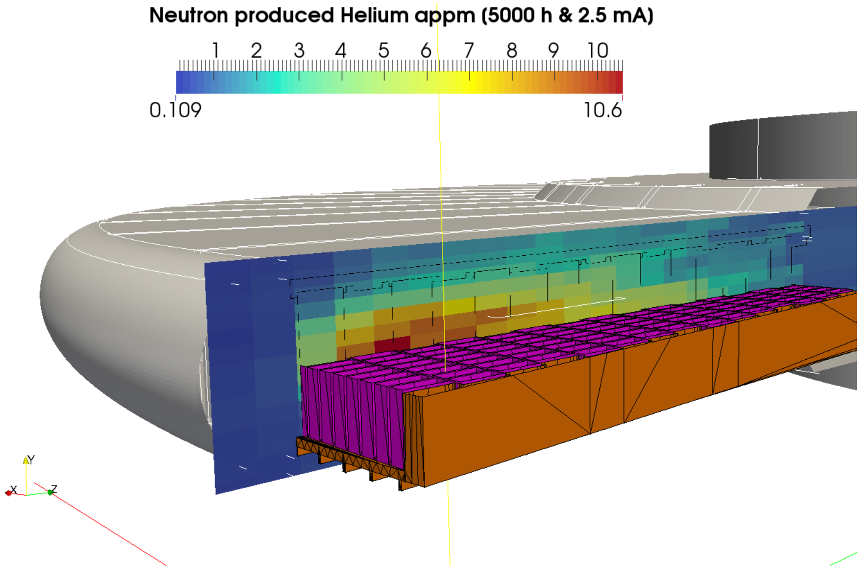

Figure 14: Helium production by neutrons in the spallation material for 5000 h full power operation

which is not a significant geometrical effect for the tungsten configuration. Regarding the damage, we should expect to have a completely brittle material after a few months of operation.

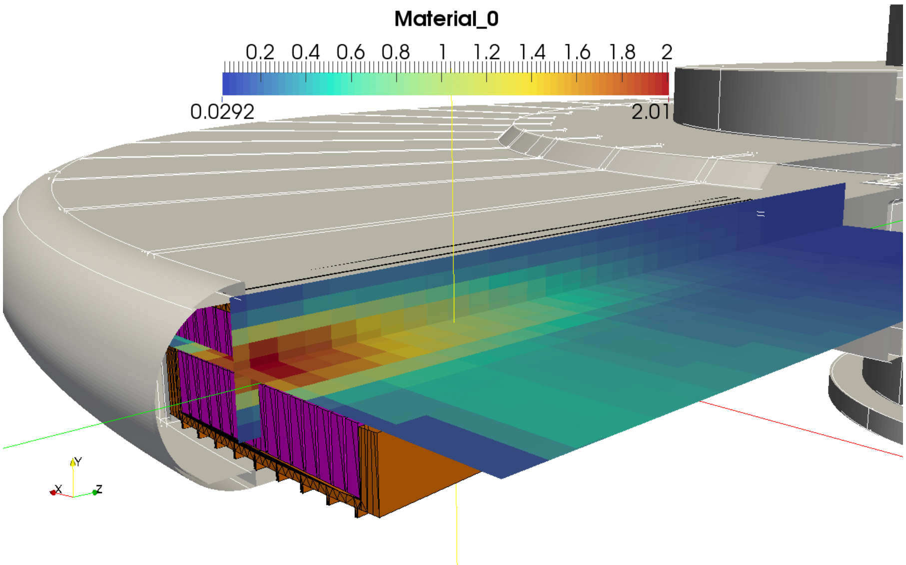

Figure 15: Total DPA in the spallation material for 5000 h full power operation

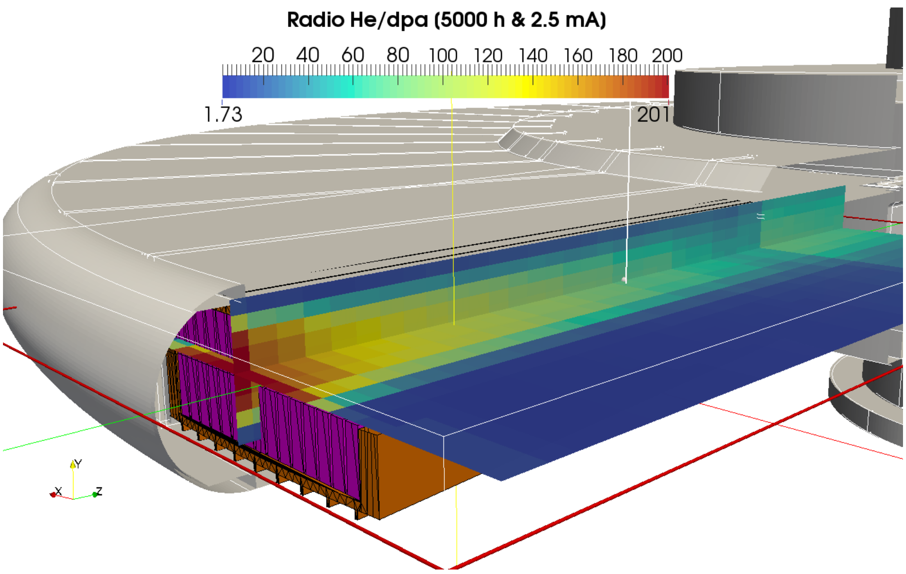

Figure 16: Ratio Helium/DPA in the spallation material for 5000 h full power operation

5.2 Damage in the target vessel

The target vessel is the structural element (material SS-316L) that configure the wheel. It has to withstand the static loads of the system (weight and helium pressure) as well as the secondary loads produced by the radiation field (temperature and thermal stress). From the nuclear safety point of view, the vessel is one of the pressurized barriers of the system and due to that it has to be designed according to the standard nuclear regulations (RCC-MRx).

In this component the only area subjected to proton flux is the beam entrance window which will be analyzer in detail in the next section. Figures 17,18 and 19 shows the neutron induced damage in the vessel elements taking into account the effect of the rotation of the wheel. In can be remark that the gas production in the component is relatively low because of the rotation of the wheel which dilutes the high energy neutrons produced on the spallation reaction with the moderated neutrons coming from the surrounded elements.

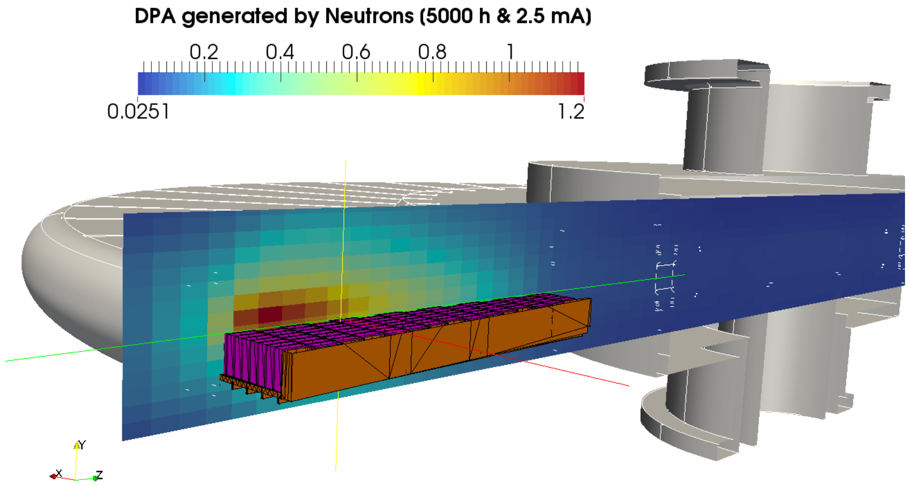

Figure 17: Neutron induced damage (DPA)in the target vessel for 5000 h full power operation

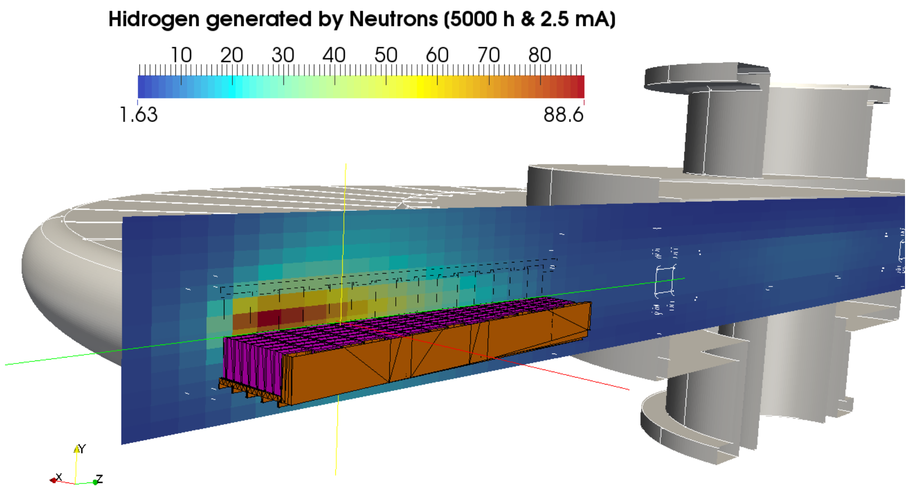

Figure 18: Hydrogen production by neutrons in the target vessel for 5000 h full power operation

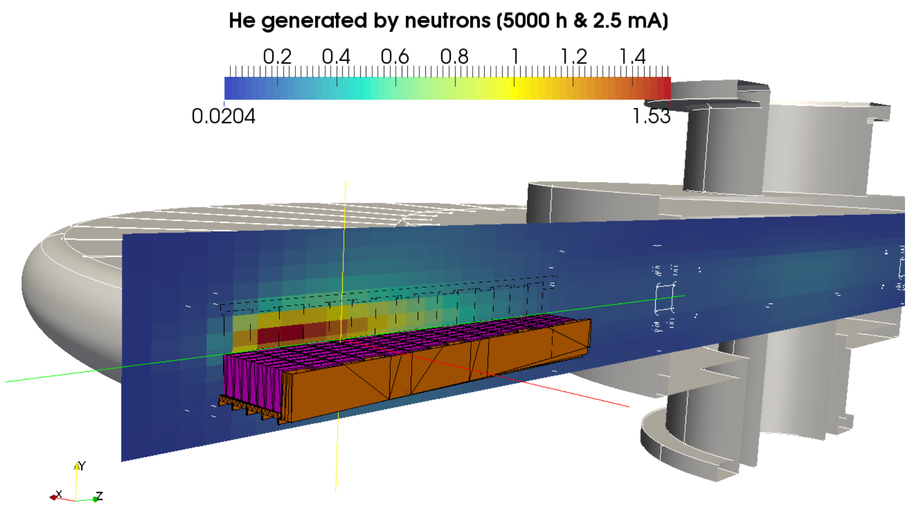

Figure 19: Helium production by neutrons in the target vessel for 5000 h full power operation

Figures 20 and 21 show the fraction of damage produced by neutrons below 14 and 30 MeV. Despite of the fact that Neutrons at high energy do not produce a damage cascade structure with sustantial differences compared with fusion neutrons, more that 85% of the displacements in the maximum of neutron damage is produced close to fusion conditions, which reinforces the argument in the Section3.4). Considering the gas production, the maximum He/dpa ratio is he range $1-2$ He-appm per dpa which is in the standard range for fision-fusion applications. Hence, the RCC-MRx limits proposed for SS-316L are valid for the Target Vessel damage conditions.

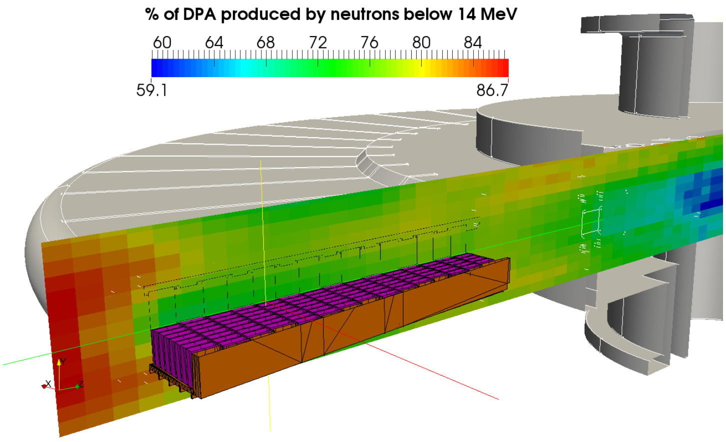

Figure 20: Fraction of DPA produced by neutrons bewlow 14 MeV

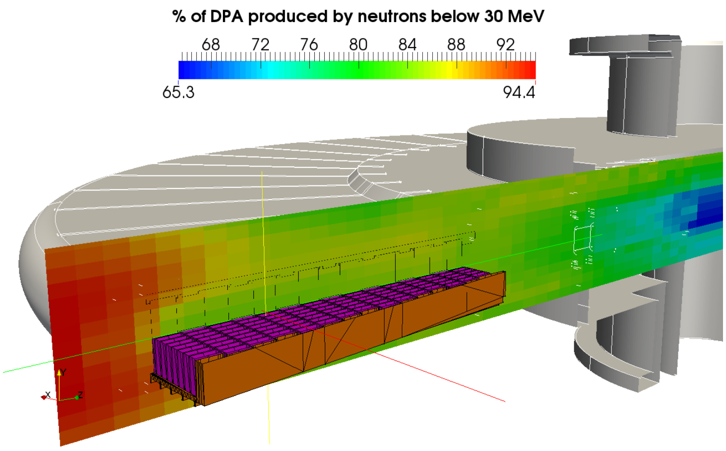

Figure 21: Fraction of DPA produced by neutrons bewlow 30 MeV

The target vessel life time is 5 years of full power operation so the maximum dpa value will be $\sim$ 6 dpa. The Table 3 shows the limits proposed by RCC-MRx code for SS-316L under radiation for secondary loads. It should be remarked that the maximum values of dpa are only produced in the center of the rib in between sectors so, the mechanical limit for other areas of the vessel can be much higher than the value included in the Table.

Temperature	200^oC	350^oC
DPA	$S_{em}^A(MPa)$	$S_{em}^A(MPa)$
2.75	2320	1857
4	1724	1376
6	771	606
6	771	606

Table 3: $S_{em}^A(MPa)$ for SS-316L proposed on RCC-MRx. In blue the DPA values for the worse position in the target vessel

5.3 Damage on the beam entrance window

The proton beam window is irradiated by neutrons generated in the spallation material and by protons of the beam so the radiation damage has these two components. Figures 22, 23 and 24 show the DPA, hidrogen and helium production in the window by the proton flux. The total DPA value is not very different from other facilities due to the dilution effect produced by the rotation because it splits the proton damage in between 36 sectors.

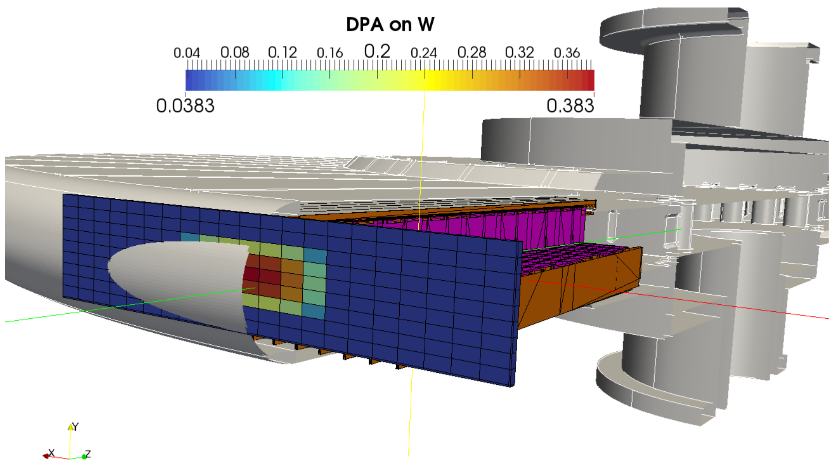

Figure 22: Proton induced damage (DPA) on the proton beam window for 5000 h full power operation

Taking into account the neutron dpa generation, the maximum damage value in the window will be 0.7 dpa year^{-1} with a He/dpa ratio in the range of 200. After 5 years of operation the window has 3.5 dpa with a gas accumulation below 700 appm, almost a factor of 2 lower than other facilities like SNS [15].

The Table 4 shows the limits proposed by RCC-MRx code for SS-316L under radiation for secondary loads. **Based on the previous discussion, we will consider the limits of secondary loads associated to 4 dpa**.

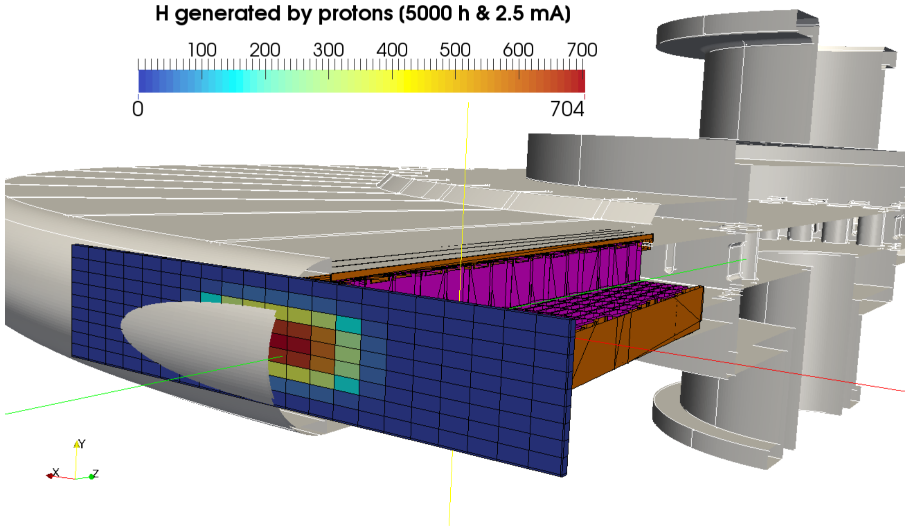

Figure 23: Hydrogen production by protons in the beam window for 5000 h full power operation

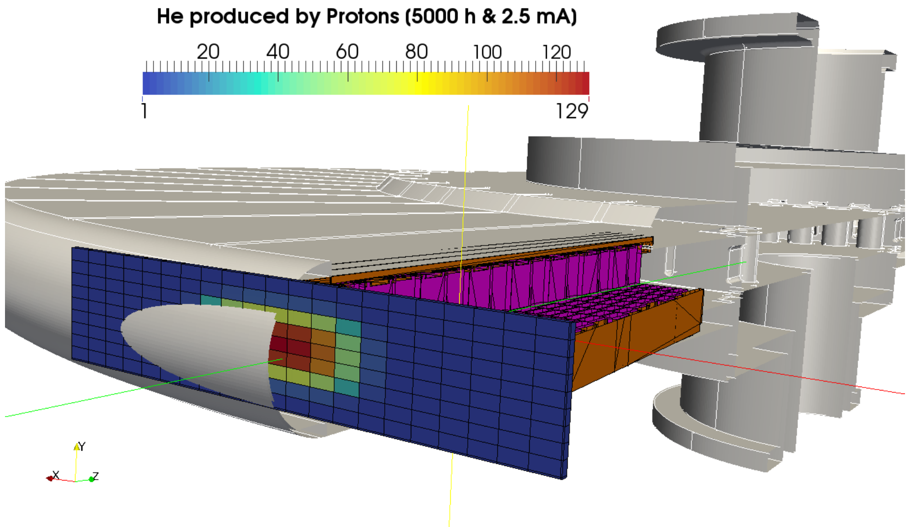

Figure 24: Helium production by protons in the beam window for 5000 h full power operation

Temperature	$200^{o}C$	$350^{o}C$
DPA	$S^{A}_{em}(MPa)$	$S^{A}_{em}(MPa)$
2.75	2320	1857
4	1724	1376
6	771	606
*4	1724	1376

Table 4: $S^{A}_{em}(MPa)$ for SS-316L proposed on RCC-MRx. In blue the DPA values for the worse position in the proton beam window

6 Conclusions

The characterization of the irradiation damage conditions for the target wheel materials has been completed. Based on this analysis the following conclusions can be remarked:

- The spallation material will accumulate 10 dpa and 2000 appm of helium after 5 years of operation. The swelling will not be significant but the material will be brittle after a few months of operation.
- The damage values produced in the target vessel are relatively moderated ($<$ 6 DPa) and its effect will be included in the RCC-MRx analysis.
- The design of the beam entrance window required the assimilation of proton to high energy neutron irradiation. After 5 years of operation the window has 3.5 dpa with a gas accumulation below 700 appm, almost a factor of 2 lower than other facilities like SNS [15].

References

[1] Konobeyev, A. Yu, U. Fischer, and L. Zanini. "New Data Files for the Calculation of Neutron and Proton Induced Radiation Damage Rates in Structural Materials of High Energy Systems."

[2] Robinson, M. T. (1994). Basic physics of radiation damage production. Journal of nuclear materials, 216, 1-28.

[3] Standard practice for neutron radiation damage simulation by charged particle irradiation. Am. Soc. Test. Matter., p 167, 1989

[4] Chadwick, M. B., Obložinský, P., Herman, M., Greene, N. M., McKnight, R. D., Smith, D. L., ... & Van der Marck, S. C. (2006). ENDF/B-VII. 0: Next generation evaluated nuclear data library for nuclear science and technology. Nuclear data sheets, 107(12), 2931-3060.

[5] Zarkadoula, E., Daraszewicz, S. L., Duffy, D. M., Seaton, M. A., Todorov, I. T., Nordlund, K., ... & Trachenko, K. (2013). The nature of high-energy radiation damage in iron. Journal of Physics: Condensed Matter, 25(12), 125402.

[6] JM. Perlado et all. JNM 1992

[7] Fernandez-Alonso, Felix, and David L. Price. Neutron Scattering. Vol. 44. Academic Press, 2013. Chapter 2, Neutron Sources by J. Bermejo,

[8] http://www.afcen.com/en/publications/rcc-mrx

[9] Pelowitz, Denise B. MCNP6 User's Manual, Version 1. Los Alamos National Laboratory, Report LA-CP-13-00634, Revision 0,(May 2013), 2013.

[10] ESS-0037286, ESS-BILBAO Target model August, 2015

[11] Wu, Y., & FDS Team. (2009). CAD-based interface programs for fusion neutron transport simulation. Fusion Engineering and Design, 84(7), 1987-1992.

[12] Grosse, D., & Fischer, U. (2012, September). The McCad Geometry Conversion Tool and Related Visualization Capabilities for 3D Neutronics Calculations. In 27th Symp. on Fusion Technology (pp. 24-28).

[13] F.J. Alonso, J. Sanz, J.M. Perlado, "Daño en materiales estructurales candidatos para un reactor comercial de fusión", DENIM 198, 1989

[14] ESS-0028465, ESS Materials Handbook

[15] McClintock, David A., Bradley J. Vevera, Bernard W. Riemer, Franz X. Gallmeier, James W. Hyres, and Phillip D. Ferguson. "Post-irradiation tensile properties of the first and second operational target modules at the Spallation Neutron Source." Journal of Nuclear Materials 450, no. 1 (2014): 130-140.